SOLUTION OF THE NAVIER-STOKES EQUATIONS IN THE THREE-DIMENSIONAL SPACE USING THE MACCORMACK ALGORITHM - PARTE II

Edisson Sávio de Góes Maciel
Rua Demócrito Cavalcanti, 152 - Afogados
Recife – PE – Brazil - CEP 50750-080
e-mail: edissonsavio@yahoo.com.br

Abstract. *The present work studies the MacCormack algorithm applied to the solution of the Navier-Stokes equations in the three-dimensional space, solving aerospace problems. A finite volume formulation is used, as also a cell centered data structure and a structured spatial discretization. The scheme is second order accurate in space and time. The time integration uses a predictor-corrector method with forward spatial discretization in the predictor step and backward spatial discretization in the corrector step. An artificial dissipation operator based on Azevedo work is implemented to guarantee the scheme numerical stability in the presence of shock waves and background instabilities. A spatially variable time step is implemented aiming to accelerate the convergence process to the steady state solution. The physical problems of the supersonic flow along a ramp and of the "cold gas" hypersonic flow along a diffuser are solved. The results have demonstrated good description of the flow fields. In the ramp problem the shock is well detected and in the diffuser problem the shock interference is well solved. A final analysis of the computational performance (cost, maximum CFL number and iterations to convergence) is accomplished.*

Keywords*: MacCormack algorithm, Navier-Stokes equations, Finite volumes, Three-dimensional space, Supersonic and hypersonic flows.*

1. Introduction

It is necessary to solve the Navier-Stokes equations in the three-dimensional space using turbulence models more precise to obtain more realistic flow properties, inside a reasonable cost interval. Direct simulations or large eddy simulation are still very expensive and require a high computational power which is still elevated to Brazil. Three-dimensional studies start with inviscid simulations, aiming to check the solver to typical problems, and, posteriorly, are intensified to the solution of the laminar Navier-Stokes equations and finally to the turbulent Navier-Stokes equations.

Pulliam and Steger (1980) performed studies with the Navier-Stokes equations, in its thin layer formulation, applied to three-dimensional flows. An implicit finite difference scheme was used to simulations of unsteady flows in configurations of arbitrary geometry through the use of a generalized coordinate system. An implicit approximated factorization technique was employed aiming to obtain better stability conditions in the solution of the viscous flows. The authors emphasized that the implemented scheme could be used to inviscid and viscous, unsteady and steady flows.

Long, Khan and Sharp (1991) developed a method to the solution of the Euler and the Navier-Stokes equations in the three-dimensional space. The method was developed in a finite volume formulation and the spatial discretization could be structured or unstructured to hexahedral or tetrahedral meshes, respectively. It was used a cell centered data structure and the time integration was performed by a Runge-Kutta method of three, four or five stages. The scheme could be symmetrical, with an artificial dissipation operator to guarantee numerical stability, or upwind. In the upwind case, it was used the Roe (1981) scheme. Tests were accomplished with Delta and Lockheed/AFOSR wings.

In the present work, the MacCormack (1969) scheme is implemented, on the context of finite volumes and using a structured spatial discretization, to solve the Navier-Stokes equations in the three-dimensional space applied to the problems of the supersonic flow along a ramp and of the "cold gas" hypersonic flow along a diffuser. The implemented scheme is second order accurate in space and time. It is necessary the introduction of a dissipation operator to guarantee the numerical stability to the scheme and the Azevedo (1992) model is implemented. The algorithm is accelerated to steady state solution using a spatially variable time step. The results have demonstrated that the MacCormack (1969) scheme supplies satisfactory solutions, detecting the main flow characteristics.

The importance of this work is to describe a numerical tool to perform numerical experiments in three-dimensions. As highlighted above, three-dimension studies are very important to describe the complex flowfield of three-dimensional physical problems of interest and a numerical tool which accomplishes this task is necessary to any CFD researcher. So, this work describes the MacCormack (1969) algorithm as a tool able to perform this task. Moreover, two numerical experiments are tested and can be used as reference experiments to CFD community.

2. Navier-Stokes equations

The fluid movement is described by the Navier-Stokes equations, which express the conservation of mass, of momentum and of energy to a viscous, heat conductor and compressible mean, in the absence of external forces. In the integral and conservative forms, these equations can be represented by:

$$\partial/\partial t \int_V Q dV + \int_S \left[\left(E_e - E_v\right) n_x + \left(F_e - F_v\right) n_y + \left(G_e - G_v\right) n_z \right] dS = 0 \,, \tag{1}$$

where Q is written to a Cartesian system; V is the cell volume; n_x, n_y and n_z are normal unity vector components to the flux face; S is the flux area; E_e, F_e and G_e are the convective flux vector components; and E_v, F_v and G_v are the diffusive flux vector components. The vectors Q, E_e, F_e, G_e, E_v, F_v and G_v are represented by:

$$Q = \begin{Bmatrix} \rho \\ \rho u \\ \rho v \\ \rho w \\ e \end{Bmatrix}, \quad E_e = \begin{Bmatrix} \rho u \\ \rho u^2 + p \\ \rho uv \\ \rho uw \\ (e+p)u \end{Bmatrix}, \quad F_e = \begin{Bmatrix} \rho v \\ \rho uv \\ \rho v^2 + p \\ \rho vw \\ (e+p)v \end{Bmatrix} \quad \text{and} \quad G_e = \begin{Bmatrix} \rho w \\ \rho uw \\ \rho vw \\ \rho w^2 + p \\ (e+p)w \end{Bmatrix}; \tag{2}$$

$$E_v = \frac{1}{Re} \begin{Bmatrix} 0 \\ \tau_{xx} \\ \tau_{xy} \\ \tau_{xz} \\ \tau_{xx} u + \tau_{xy} v + \tau_{xz} w - q_x \end{Bmatrix}, \; F_v = \frac{1}{Re} \begin{Bmatrix} 0 \\ \tau_{yx} \\ \tau_{yy} \\ \tau_{yz} \\ \tau_{yx} u + \tau_{yy} v + \tau_{yz} w - q_y \end{Bmatrix} \text{ and } G_v = \frac{1}{Re} \begin{Bmatrix} 0 \\ \tau_{zx} \\ \tau_{zy} \\ \tau_{zz} \\ \tau_{zx} u + \tau_{zy} v + \tau_{zz} w - q_z \end{Bmatrix}. \tag{3}$$

In these equations, the components of the viscous stress tensor are defined as:

$$\tau_{xx} = 2\mu \frac{\partial u}{\partial x} - \frac{2}{3}\mu \left(\frac{\partial u}{\partial x} + \frac{\partial v}{\partial y} + \frac{\partial w}{\partial z} \right), \; \tau_{xy} = \mu \left(\frac{\partial u}{\partial y} + \frac{\partial v}{\partial x} \right), \; \tau_{xz} = \mu \left(\frac{\partial u}{\partial z} + \frac{\partial w}{\partial x} \right),$$
$$\tau_{yy} = 2\mu \frac{\partial v}{\partial y} - \frac{2}{3}\mu \left(\frac{\partial u}{\partial x} + \frac{\partial v}{\partial y} + \frac{\partial w}{\partial z} \right), \; \tau_{zz} = 2\mu \frac{\partial w}{\partial z} - \frac{2}{3}\mu \left(\frac{\partial u}{\partial x} + \frac{\partial v}{\partial y} + \frac{\partial w}{\partial z} \right) \text{ and } \tau_{yz} = \mu \left(\frac{\partial v}{\partial z} + \frac{\partial w}{\partial y} \right). \tag{4}$$

The components of the conducted heat flux vector are defined by the Fourier law as follows:

$$q_x = -\left(\frac{\gamma \mu}{Pr} \right) \frac{\partial e_i}{\partial x}, \quad q_y = -\left(\frac{\gamma \mu}{Pr} \right) \frac{\partial e_i}{\partial y} \quad \text{and} \quad q_z = -\left(\frac{\gamma \mu}{Pr} \right) \frac{\partial e_i}{\partial z}, \tag{5}$$

where ρ is the fluid density; u, v and w are the Cartesian components of the velocity vector in the x, y and z directions, respectively; e is the total energy per unity volume; p is the static pressure; μ represents the fluid molecular viscosity; Prd is the laminar Prandtl number; γ is the ratio of specific heats; Re is the flow Reynolds number; and e_i is the fluid internal energy, defined as

$$e_i = e/\rho - 0.5\left(u^2 + v^2 + w^2\right). \tag{6}$$

The Navier-Stokes equations were nondimensionalized in relation to the freestream density, ρ_∞, the freestream speed of sound, a_∞, and the freestream molecular viscosity, μ_∞, for the studied problems. The matrix system of the Navier-Stokes equations is closed with the state equation of a perfect gas:

$$p = (\gamma - 1)\left[e - 0.5\rho(u^2 + v^2 + w^2) \right]. \tag{7}$$

3. MacCormack (1969) algorithm

Using the Green theorem in Equation (1) and adopting a structured mesh notation to the fluid properties and of the flow, it is possible to write that:

$$\partial Q_{i,j,k} / \partial t = -1/V_{i,j,k} \int_{S_{i,j,k}} (\vec{P} \cdot \vec{n})_{i,j,k} \, dS_{i,j,k} \,, \tag{8}$$

with $\vec{P} = \left[\left(E_e - E_v\right) \; \left(F_e - F_v\right) \; \left(G_e - G_v\right) \right]^t$, being the convective and the diffusive flux vector. A given

computational cell in this notation is formed by the following nodes: *(i,j,k)*, *(i+1,j,k)*, *(i+1,j+1,k)*, *(i,j+1,k)*, *(i,j,k+1)*, *(i+1,j,k+1)*, *(i+1,j+1,k+1)* and *(i,j+1,k+1)*. Details of this representation are available in Maciel (2002) and in Maciel (2004). The calculation of the computational cell volumes is based, in the more general case, on the determination of the volume of one deformed hexahedral in three-dimensional space. The formation of the hexahedral, as well as the vertex nodes which define each cell, can be found in details in Maciel (2002) and in Maciel (2004). In Maciel (2002) is also found details of the calculation of a given hexahedral volume.

The hexaedral flux area is calculated by the sum of the half areas defined by the norm of the external products $\left|\vec{a}\,x\,\vec{b}\right|$ and $\left|\vec{c}\,x\,\vec{d}\right|$, where $\vec{a}$, $\vec{b}$, $\vec{c}$ and $\vec{d}$ are vectors formed by the nodes which define a given flux surface, as described in Maciel (2002) and in Maciel (2004). The physical quantity $0.5\left(\left|\vec{a}\,x\,\vec{b}\right|+\left|\vec{c}\,x\,\vec{d}\right|\right)$ determines the flux area of each face, which is the area of a deformed rectangle.

The explicit time march, using the explicit Euler method applied to Eq. (8), leads to the following expression:

$$Q_{i,j,k}^{n+1} = Q_{i,j,k}^{n} - \Delta t / V_{i,j,k} \int_{S_{i,j,k}} (\vec{P}\cdot\vec{n})_{i,j,k}\, dS_{i,j,k} \quad . \tag{9}$$

In the discretization of the surface integral, the Eq. (9) can be rewritten as:

$$Q_{i,j,k}^{n+1} = Q_{i,j,k}^{n} - \Delta t / V_{i,j,k} \left[(\vec{P}\cdot\vec{S})_{i,j-1/2,k} + (\vec{P}\cdot\vec{S})_{i+1/2,j,k} + (\vec{P}\cdot\vec{S})_{i,j+1/2,k} + (\vec{P}\cdot\vec{S})_{i-1/2,j,k} + (\vec{P}\cdot\vec{S})_{i,j,k-1/2} + (\vec{P}\cdot\vec{S})_{i,j,k+1/2} \right]^{n} , \tag{10}$$

where , for example, $\vec{S}_{i,j-1/2,k}$ has the direction and the orientation of the $\vec{n}_{i,j-1/2,k}$ and magnitude equals to the area value $S_{i,j-1/2,k}$. The half indexes indicate fluxes calculated in the respective faces or cell surfaces.

To the calculation of the viscous flux vectors, the derivatives present in Eqs. (4) and (5) are considered constants to a given volume and calculated in terms of the property surface integral along the control volume faces (Green theorem):

$$\frac{\partial u}{\partial x} = \frac{1}{V}\int_V \frac{\partial u}{\partial x}\, dV = \frac{1}{V}\int_S u\left(\vec{n}_x \bullet d\vec{S}\right) = \frac{1}{V}\int_{S_x} u\, dS_x \cong \frac{1}{V}\sum_{l=1}^{6} u_{i,j,k_l} S_{xi,j,k_l} \quad , \tag{11}$$

$$\frac{\partial v}{\partial y} = \frac{1}{V}\int_V \frac{\partial v}{\partial y}\, dV = \frac{1}{V}\int_S v\left(\vec{n}_y \bullet d\vec{S}\right) = \frac{1}{V}\int_{S_y} v\, dS_y \cong \frac{1}{V}\sum_{l=1}^{6} v_{i,j,k_l} S_{yi,j,k_l} \quad , \tag{12}$$

$$\frac{\partial w}{\partial z} = \frac{1}{V}\int_V \frac{\partial w}{\partial z}\, dV = \frac{1}{V}\int_S w\left(\vec{n}_z \bullet d\vec{S}\right) = \frac{1}{V}\int_{S_z} w\, dS_z \cong \frac{1}{V}\sum_{l=1}^{6} w_{i,j,k_l} S_{zi,j,k_l} \quad , \tag{13}$$

where, for example, u_{i,j,k_l} is the arithmetical average between cell (i,j,k) and its respective neighbor. The value of the derivative $\partial u/\partial x$ at flux interface *(i,j-1/2,k)*, for example, is adopted as being $\partial u/\partial x$ of the volume *(i,j,k)* in the predictor step and as being $\partial u/\partial x$ of volume *(i,j-1,k)* in the corrector step.

- Predictor step:

$$\begin{aligned}
\Delta Q_{i,j,k}^{n} = -\frac{\Delta t}{V_{i,j,k}} \Big\{ & \left[(E_e - E_v) n_{x\,i,j-1/2,k} + (F_e - F_v) n_{y\,i,j-1/2,k} + (G_e - G_v) n_{z\,i,j-1/2,k} \right]_{i,j,k} S_{i,j-1/2,k} + \\
& \left[(E_e - E_v) n_{x\,i+1/2,j,k} + (F_e - F_v) n_{y\,i+1/2,j,k} + (G_e - G_v) n_{z\,i+1/2,j,k} \right]_{i+1,j,k} S_{i+1/2,j,k} + \\
& \left[(E_e - E_v) n_{x\,i,j+1/2,k} + (F_e - F_v) n_{y\,i,j+1/2,k} + (G_e - G_v) n_{z\,i,j+1/2,k} \right]_{i,j+1,k} S_{i,j+1/2,k} + \\
& \left[(E_e - E_v) n_{x\,i-1/2,j,k} + (F_e - F_v) n_{y\,i-1/2,j,k} + (G_e - G_v) n_{z\,i-1/2,j,k} \right]_{i,j,k} S_{i-1/2,j,k} + \\
& \left[(E_e - E_v) n_{x\,i,j,k-1/2} + (F_e - F_v) n_{y\,i,j,k-1/2} + (G_e - G_v) n_{z\,i,j,k-1/2} \right]_{i,j,k} S_{i,j,k-1/2} + \\
& \left[(E_e - E_v) n_{x\,i,j,k+1/2} + (F_e - F_v) n_{y\,i,j,k+1/2} + (G_e - G_v) n_{z\,i,j,k+1/2} \right]_{i,j,k+1} S_{i,j,k+1/2} \Big\} \quad ,
\end{aligned} \tag{14}$$

$$Q_{p}{}_{i,j,k}^{n+1} = Q_{i,j,k}^{n} + \Delta Q_{i,j,k}^{n} \quad .$$

- Corrector step:

$$
\begin{aligned}
\Delta Q_{c\,i,j,k}^{\,n+1} = -\frac{\Delta t}{V_{i,j,k}} \Big\{ & \Big[(E_e - E_v) n_{x\,i,j-1/2,k} + (F_e - F_v) n_{y\,i,j-1/2,k} + (G_e - G_v) n_{z\,i,j-1/2,k} \Big]_{i,j-1,k}^{p} S_{i,j-1/2,k} + \\
& \Big[(E_e - E_v) n_{x\,i+1/2,j,k} + (F_e - F_v) n_{y\,i+1/2,j,k} + (G_e - G_v) n_{z\,i+1/2,j,k} \Big]_{i,j,k}^{p} S_{i+1/2,j,k} + \\
& \Big[(E_e - E_v) n_{x\,i,j+1/2,k} + (F_e - F_v) n_{y\,i,j+1/2,k} + (G_e - G_v) n_{z\,i,j+1/2,k} \Big]_{i,j,k}^{p} S_{i,j+1/2,k} + \\
& \Big[(E_e - E_v) n_{x\,i-1/2,j,k} + (F_e - F_v) n_{y\,i-1/2,j,k} + (G_e - G_v) n_{z\,i-1/2,j,k} \Big]_{i-1,j,k}^{p} S_{i-1/2,j,k} + \\
& \Big[(E_e - E_v) n_{x\,i,j,k-1/2} + (F_e - F_v) n_{y\,i,j,k-1/2} + (G_e - G_v) n_{z\,i,j,k-1/2} \Big]_{i,j,k-1}^{p} S_{i,j,k-1/2} + \\
& \Big[(E_e - E_v) n_{x\,i,j,k+1/2} + (F_e - F_v) n_{y\,i,j,k+1/2} + (G_e - G_v) n_{z\,i,j,k+1/2} \Big]_{i,j,k}^{p} S_{i,j,k+1/2} \Big\} \quad , \\
Q_{i,j,k}^{n+1} = & \frac{1}{2} \left(Q_{i,j,k}^{n} + Q_{p\,i,j,k}^{\,n+1} + \Delta Q_{c\,i,j,k}^{\,n+1} \right) \quad .
\end{aligned}
\tag{15}
$$

Discretizing space and time together, following a Lax-Wendroff type method, dividing the resultant algorithm in two integration time steps (one predictor and the other corrector) and adopting a forward spatial discretization to the predictor step and a backward spatial discretization to the corrector step, it is possible to obtain the MacCormack (1969) algorithm, based on a finite volume formulation, as described above.

An artificial dissipation operator of second and fourth differences (Maciel and Azevedo, 1998a) is subtracted from the RHS flux terms in the corrector step, aiming to provide numerical stability in the proximities of shock waves and of uncoupled solutions.

3.1. Artificial dissipation operator

The artificial dissipation operator implemented in the MacCormack (1969) code to simulate three-dimensional flows follows the structure bellow:

$$
D\left(Q_{i,j,k}\right) = d^{(2)}\left(Q_{i,j,k}\right) - d^{(4)}\left(Q_{i,j,k}\right) \, , \tag{16}
$$

where:

$$
\begin{aligned}
d^{(2)}\left(Q_{i,j,k}\right) = & \varepsilon_{i,j,k,1}^{(2)} \frac{\left(A_{i,j,k} + A_{i,j-1,k}\right)}{2} \left(Q_{i,j-1,k} - Q_{i,j,k}\right) + \varepsilon_{i,j,k,2}^{(2)} \frac{\left(A_{i,j,k} + A_{i+1,j,k}\right)}{2} \left(Q_{i+1,j,k} - Q_{i,j,k}\right) \\
& + \varepsilon_{i,j,k,3}^{(2)} \frac{\left(A_{i,j,k} + A_{i,j+1,k}\right)}{2} \left(Q_{i,j+1,k} - Q_{i,j,k}\right) + \varepsilon_{i,j,k,4}^{(2)} \frac{\left(A_{i,j,k} + A_{i-1,j,k}\right)}{2} \left(Q_{i-1,j,k} - Q_{i,j,k}\right) \\
& + \varepsilon_{i,j,k,5}^{(2)} \frac{\left(A_{i,j,k} + A_{i,j,k-1}\right)}{2} \left(Q_{i,j,k-1} - Q_{i,j,k}\right) + \varepsilon_{i,j,k,6}^{(2)} \frac{\left(A_{i,j,k} + A_{i,j,k+1}\right)}{2} \left(Q_{i,j,k+1} - Q_{i,j,k}\right),
\end{aligned}
\tag{17}
$$

named undivided Laplacian operator, is responsible to the numerical stability in the presence of shock waves;

$$
\begin{aligned}
d^{(4)}\left(Q_{i,j,k}\right) = & \varepsilon_{i,j,k,1}^{(4)} \frac{\left(A_{i,j,k} + A_{i,j-1,k}\right)}{2} \left(\nabla^2 Q_{i,j-1,k} - \nabla^2 Q_{i,j,k}\right) + \varepsilon_{i,j,k,2}^{(4)} \frac{\left(A_{i,j,k} + A_{i+1,j,k}\right)}{2} \left(\nabla^2 Q_{i+1,j,k} - \nabla^2 Q_{i,j,k}\right) \\
& + \varepsilon_{i,j,k,3}^{(4)} \frac{\left(A_{i,j,k} + A_{i,j+1,k}\right)}{2} \left(\nabla^2 Q_{i,j+1,k} - \nabla^2 Q_{i,j,k}\right) + \varepsilon_{i,j,k,4}^{(4)} \frac{\left(A_{i,j,k} + A_{i-1,j,k}\right)}{2} \left(\nabla^2 Q_{i-1,j,k} - \nabla^2 Q_{i,j,k}\right) \\
& + \varepsilon_{i,j,k,5}^{(4)} \frac{\left(A_{i,j,k} + A_{i,j,k-1}\right)}{2} \left(\nabla^2 Q_{i,j,k-1} - \nabla^2 Q_{i,j,k}\right) + \varepsilon_{i,j,k,6}^{(4)} \frac{\left(A_{i,j,k} + A_{i,j,k+1}\right)}{2} \left(\nabla^2 Q_{i,j,k+1} - \nabla^2 Q_{i,j,k}\right),
\end{aligned}
\tag{18}
$$

named biharmonic operator, is responsible by the background stability. The following term

$$
\nabla^2 Q_{i,j,k} = \left[\left(Q_{i,j-1,k} - Q_{i,j,k}\right) + \left(Q_{i+1,j,k} - Q_{i,j,k}\right) + \left(Q_{i,j+1,k} - Q_{i,j,k}\right) + \left(Q_{i-1,j,k} - Q_{i,j,k}\right) + \left(Q_{i,j,k-1} - Q_{i,j,k}\right) + \left(Q_{i,j,k+1} - Q_{i,j,k}\right) \right] \tag{19}
$$

is named Laplacian of $Q_{i,j,k}$. In the operator $d^{(4)}$, $\nabla^2 Q_{i,j,k}$ is extrapolated from its real neighbor every time that it represents a special boundary cell, recognized in the literature as "ghost" cell. The ε terms are defined as follows:

$$\varepsilon^{(2)}_{i,j,k,1} = K^{(2)} MAX\left(\nu_{i,j,k}, \nu_{i,j-1,k}\right),\ \varepsilon^{(2)}_{i,j,k,2} = K^{(2)} MAX\left(\nu_{i,j,k}, \nu_{i+1,j,k}\right),\ \varepsilon^{(2)}_{i,j,k,3} = K^{(2)} MAX\left(\nu_{i,j,k}, \nu_{i,j+1,k}\right),$$
$$\varepsilon^{(2)}_{i,j,k,4} = K^{(2)} MAX\left(\nu_{i,j,k}, \nu_{i-1,j,k}\right),\ \varepsilon^{(2)}_{i,j,k,5} = K^{(2)} MAX\left(\nu_{i,j,k}, \nu_{i,j,k-1}\right) \text{ and } \varepsilon^{(2)}_{i,j,k,6} = K^{(2)} MAX\left(\nu_{i,j,k}, \nu_{i,j,k+1}\right); \quad (20)$$

$$\varepsilon^{(4)}_{i,j,k,1} = MAX\left[0, \left(K^{(4)} - \varepsilon^{(2)}_{i,j,k,1}\right)\right],\ \varepsilon^{(4)}_{i,j,k,2} = MAX\left[0, \left(K^{(4)} - \varepsilon^{(2)}_{i,j,k,2}\right)\right],\ \varepsilon^{(4)}_{i,j,k,3} = MAX\left[0, \left(K^{(4)} - \varepsilon^{(2)}_{i,j,k,3}\right)\right],$$
$$\varepsilon^{(4)}_{i,j,k,4} = MAX\left[0, \left(K^{(4)} - \varepsilon^{(2)}_{i,j,k,4}\right)\right],\ \varepsilon^{(4)}_{i,j,k,5} = MAX\left[0, \left(K^{(4)} - \varepsilon^{(2)}_{i,j,k,5}\right)\right] \text{ and } \varepsilon^{(4)}_{i,j,k,6} = MAX\left[0, \left(K^{(4)} - \varepsilon^{(2)}_{i,j,k,6}\right)\right], \quad (21)$$

where:

$$\nu_{i,j,k} = \frac{\left|p_{i+1,j,k} - p_{i,j,k}\right| + \left|p_{i,j+1,k} - p_{i,j,k}\right| + \left|p_{i-1,j,k} - p_{i,j,k}\right| + \left|p_{i,j,k-1} - p_{i,j,k}\right| + \left|p_{i,j-1,k} - p_{i,j,k}\right| + \left|p_{i,j,k+1} - p_{i,j,k}\right|}{p_{i,j-1,k} + p_{i+1,j,k} + p_{i,j+1,k} + p_{i-1,j,k} + p_{i,j,k-1} + p_{i,j,k+1} + 6\,p_{i,j,k}} \quad (22)$$

represents a pressure sensor, responsible by the identification of regions of high gradients. The constants $K^{(2)}$ and $K^{(4)}$ has typical values of 1/4 and 3/256, respectively. Every time that a neighbor represents a ghost cell, it is assumed that, for example, $\nu_{i,j-1,k} = \nu_{i,j,k}$. The $A_{i,j,k}$ coefficient was implemented as proposed by Azevedo (1992) and is defined as:

$$A_{i,j,k} = V_{i,j,k} / \Delta t_{i,j,k} \ . \quad (23)$$

3.2. Spatially variable time step

The idea of a spatially variable time step consists in keeping constant a CFL number in the calculation domain and to guarantee time steps appropriated to each mesh region during the convergence process. Details of this implementation is available in Maciel (2002) and in Maciel (2004).

3.3. Initial and boundary conditions

3.3.1. Initial condition

The initial condition adopted to the problems is the freestream flow in all calculation domain (Jameson and Mavriplis, 1986, Maciel, 2002, and Maciel, 2004).

3.3.2. Boundary conditions

The different types of implemented boundary conditions are described as follows.

a) Wall - The velocity components *u*, *v* and *w* of the ghost volumes are equaled to the respective values of *u*, *v* and *w* of the neighbor real volumes, with opposite signal, to the Navier-Stokes case.

$$u_g = -u_{real}\ ,\ v_g = -v_{real} \text{ and } w_g = -w_{real}\ . \quad (24)$$

The fluid pressure gradient in the direction normal to the wall is equal to zero for the viscous case. The temperature gradient is equal to zero along all wall, with this last situation according to the physical results, without impose, however, the condition of adiabatic wall. With these two conditions, a zero order extrapolation is performed to the pressure and to the temperature. It is also concluded that the fluid density is obtained by zero order extrapolation.

b) Far field - In the implementation of the boundary conditions in the mesh limit external region to physical problems of external flow, it is necessary to identify four possible situations: entrance with subsonic flow, entrance with supersonic flow, exit with subsonic flow and exit with supersonic flow. These situations are described bellow.

b.1) Entrance with subsonic flow – Considering the one-dimensional characteristic relation concept in the normal direction of flow penetration, the entrance with subsonic flow presents four characteristic velocities of information propagation which have direction and orientation point inward the calculation domain, which implies that the variables associated with these waves can not be extrapolated (Maciel and Azevedo, 1997, Maciel and Azevedo, 1998b, Maciel, 2002, and Maciel, 2004). It is necessary to specify four conditions to these four information. Jameson and Mavriplis (1986) indicate as appropriated quantities to be specified the freestream density and the freestream Cartesian velocity components *u*, *v* and *w*. Just the last characteristics, "*(q_n-a)*", which transports information from inside to outside of the calculation domain, can not be specified and will have to be determined by interior information of the calculation

domain. In this work, a zero order extrapolation to the pressure is performed, being the total energy defined by the state equation of a perfect gas.

b.2) Entrance with supersonic flow - All variables are specified in the entrance boundary, adopting freestream values.

b.3) Exit with subsonic flow - Four characteristics which govern the Euler equations proceed from the internal region of the calculation domain. So, the density and the Cartesian velocity components are extrapolated from the interior domain. One condition should be specified to the boundary. In this case, the pressure is fixed in the calculation domain exit, keeping its respective value of freestream flow.

b.4) Exit with supersonic flow - The five characteristics which govern the Euler equations proceed from the internal region of the calculation domain. It is not possible to specify variable values at the exit. The zero order extrapolation is applied to density, Cartesian velocity components and pressure.

c) Entrance and exit – The entrance and exit boundaries are applied to both problems. Boundary conditions which involve flow entrance in the calculation domain had the flow properties fixed with freestream values. Boundary conditions which involve flow exit of the computational domain used simply the zero order extrapolation to the determination of properties in this boundary. This procedure is correct because the entrance flow and the exit flow are no minimal supersonic to both studied examples.

6. Results

Tests were accomplished in an ATHLON-2.6GHz and 64 Mbytes of RAM memory microcomputer. Converged results occurred to 4 orders of reduction in the maximum residual value. The value used to γ was 1.4. The configuration downstream and the configuration longitudinal plane angles were set equal to 0.0°.

The ramp problem is a supersonic flow hitting a ramp with 20° of inclination. It originates a shock wave and an expansion fan. In the diffuser problem, it occurs the interference between the two shocks originated from the lower and upper wall. This interference occurs at the throat of the diffuser.

6.1. Ramp physical problem

The algebraic mesh used in this problem has 42,660 real volumes and 48,800 nodes to the structured calculation domain. It is equivalent to a mesh with 61 points in the ξ direction, 80 points in the η direction and 10 points in the ς direction. To this physical problem, ramp with 20º of inclination, was adopted a freestream Mach number equals to 5.0 as initial condition. It was considered a flight altitude of 20,000 meters and the ramp characteristic length assumed the value 0.044 meter. The altitude supplies values of density, pressure and viscosity and, hence, it is possible to determine the Reynolds number of this simulation, which was 403,143.7.

Figures 1, 2 and 3 show the density, the pressure and the Mach number contours, respectively, obtained to this configuration with the MacCormack (1969) scheme. They do not present pre-shock oscillations, typical of the second order accurate schemes, and all figures have good symmetry properties in the z-planes.

Figure 4 show –Cp distribution obtained along the ramp, in the section k = kmax/2, where “kmax” represents the maximum number of point in the z direction. The shock and the expansion fan are well detected, but the shock is smoothed in relation to the expected solution.

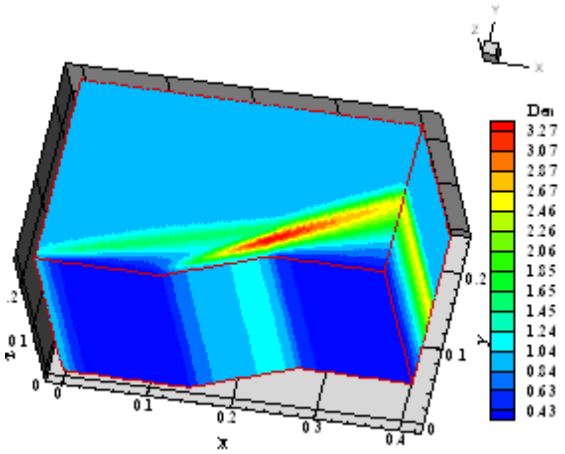

Figure 1 – Density field.

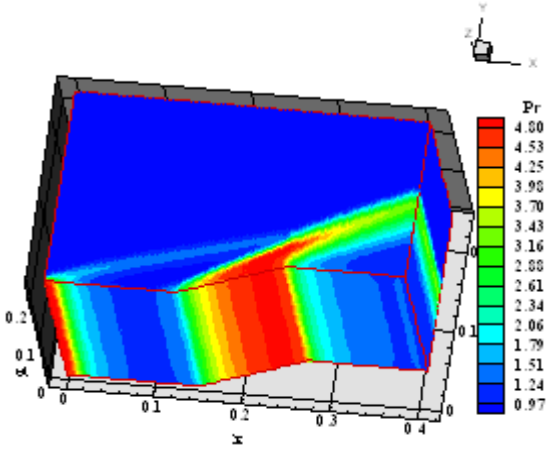

Figure 2 – Pressure field.

The CFL number used in this viscous simulation, with the MacCormack (1969) scheme, was 0.1 and the number of iterations to convergence was 15,806. The computational cost of the MacCormack (1969) scheme was 0.0000858s/per volume/per iteration.

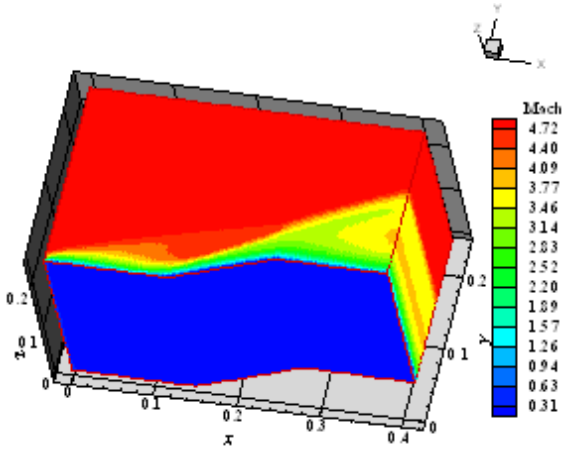

Figure 3. Mach number field.

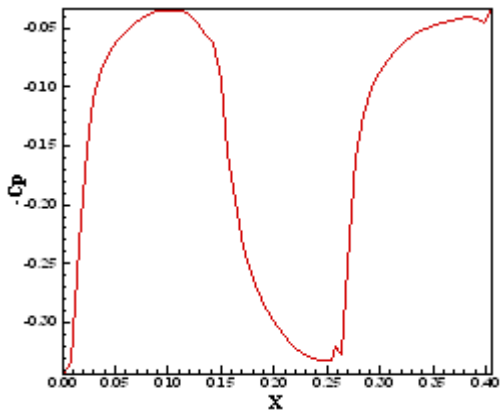

Figure 4. -Cp distribution.

6.2. Diffuser physical problem

The mesh to this problem has 32,400 real volumes and 37,210 nodes to the structured discretization of the calculation domain. It is equivalent to a mesh with 61 points in the ξ direction, 61 points in the η direction and 10 points in the ς direction. The initial condition to this problem, involving a diffuser with 20º of inclination, adopted a freestream Mach number of 10.0 and flight altitude of 40,000 meters. The diffuser characteristic length was 0.21 meter and the Reynolds number of this simulation was calculated in 166,312.48.

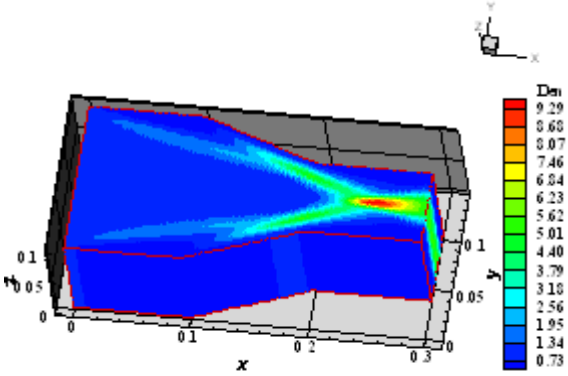

Figure 5. Density field.

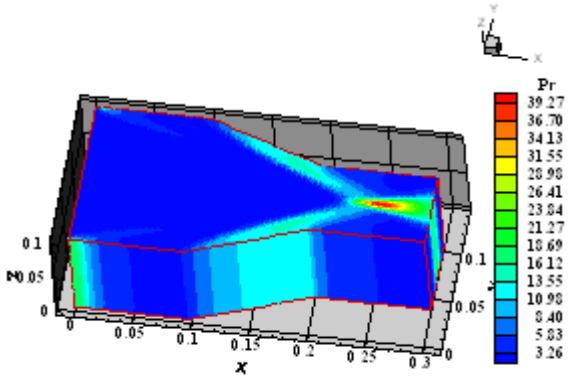

Figure 6. Pressure field.

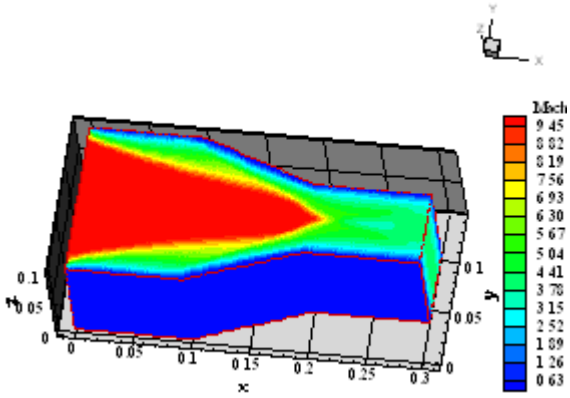

Figure 7. Mach number field.

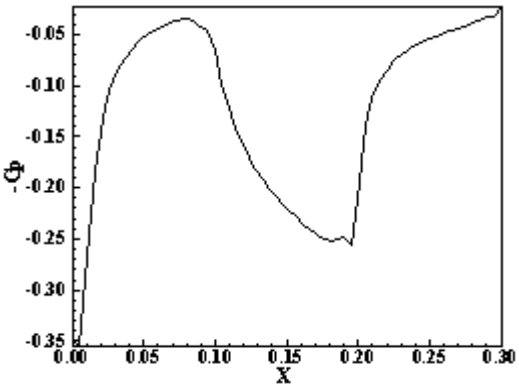

Figure 8. -Cp distribution.

Figures 5, 6 and 7 present the density, pressure and Mach number contours, respectively, obtained by the MacCormack (1969) numerical scheme to this viscous simulation. Figures 6 and 7 show good symmetry characteristics in the y- and z-planes and the shock intersection involving the shock of the upper wall and the shock of the lower wall is well highlighted. The Mach number contours in Fig. 7 do not present pre-shock oscillations.

Figure 8 shows the -Cp distribution along the diffuser lower wall, in the section k = kmax/2. In this Figure, the region of the beginning of the diffuser presents a smoothed -Cp distribution, after that appears what should be the shock

and finally, at the ramp end, appears the expansion fan. The shock and the expansion fan are highly smoothed. The CFL used in this simulation was 0.1 and the number of iterations to convergence was 14,311.

7. Conclusions

This work presented the MacCormack (1969) algorithm implemented in its version to three-dimensions. The algorithm is explicit, second order accurate in space and time and integrated in time in two steps: a predictor step, with forward spatial discretization, and a corrector step, with backward spatial discretization. The Navier-Stokes equations were solved, using a finite volume formulation, with a cell centered data base and structured spatial discretization. The supersonic flow along a ramp and the "cold gas" hypersonic flow along a diffuser were solved. A spatially variable time step was implemented to accelerate the convergence process to the steady state condition.

The obtained results were of good quality, do not occurring pre-shock oscillations in the Mach number contours. The density and the pressure fields presented good behavior highlighting well the shock in the ramp problem and detecting appropriately the shock interference in the diffuser problem. The -Cp distribution shows well the shock and the expansion fan in both problems. The computational cost of the present implementation was 0.0000858s/per volume/per iteration.

8. Acknowledgements

The author thanks the financial support conceded by CNPq under the form of scholarship of process number 304318/2003-5, DCR/1F.

9. References

Azevedo, J. L. F., 1992, "On the Development of Unstructured Grid Finite Volume Solvers for High Speed Flows", NT-075-ASE-N, IAE, CTA, São José dos Campos, SP.

Jameson, A. and Mavriplis, D., 1986, "Finite Volume Solution of the Two-Dimensional Euler Equations on a Regular Triangular Mesh", AIAA Journal, Vol. 24, No. 4, pp. 611-618.

Long, L. N, Khan, M. M. S., and Sharp, H. T., 1991, "Massively Parallel Three-Dimensional Euler / Navier-Stokes Method", AIAA Journal, Vol. 29, No. 3, pp. 657-666.

MacCormack, R. W., 1969, "The Effect of Viscosity in Hypervelocity Impact Cratering", AIAA Paper 69-354.

Maciel, E. S. G. and Azevedo, J. L. F., 1997, "Comparação entre Vários Algoritmos de Fatoração Aproximada na Solução das Equações de Navier-Stokes", Proceedings of the 14th Brazilian Congress of Mechanical Engineering (available in CD-ROM), Bauru, SP, Brasil.

Maciel, E. S. G., and Azevedo, J. L. F., 1998a, "Comparação entre Vários Modelos de Dissipação Artificial na Solução das Equações de Navier-Stokes", Proceedings of the V Congress of Machenical Engineering North-Northest (V CEM-NNE), Vol. 3, Fortaleza, CE, pp. 604-611.

Maciel, E. S. G. and Azevedo, J. L. F., 1998b, "Comparação entre Vários Esquemas Implícitos de Fatoração Aproximada na Solução das Equações de Navier-Stokes", RBCM- Journal of the Brazilian Society of Mechanical Sciences, Vol. XX, No. 3, pp. 353-380.

Maciel, E. S. G., 2002, "Simulação Numérica de Escoamentos Supersônicos e Hipersônicos Utilizando Técnicas de Dinâmica dos Fluidos Computacional", Doctoral thesis, ITA, CTA, São José dos Campos, SP, Brazil, 258 p.

Maciel, E. S. G., 2004, "Relatório ao Conselho Nacional de Pesquisa e Desenvolvimento Tecnológico (CNPq) sobre as Atividades de Pesquisa Desenvolvidas no Primeiro Ano de Vigência da Bolsa de Estudos para Nível DCR-IF Referente ao Processo nº 304318/2003-5", Technical report to CNPq, November, 37 p.

Pulliam, T. H., and Steger, J. L., 1980, "Implicit Finite-Difference Simulations of three-Dimensional Compressible Flow", AIAA Journal, Vol. 18, No. 2, pp. 159-166.

Roe, P. L., 1981, "Approximate Riemann Solvers, Parameter Vectors, and Difference Schemes", Journal of Computational Physics, Vol. 43, pp. 357-372.

10. Responsibility notice

The author is the only responsible for the printed material included in this paper.